

Local vibration at the surface of a Ge nanocrystal embedded in a silicon oxide matrix

Y. M. Yang, X. L. Wu,^{a)} L. W. Yang, G. S. Huang, T. Qiu, and Y. Shi
*National Laboratory of Solid State Microstructures and Department of Physics, Nanjing University,
 Nanjing 210093, People's Republic of China*

G. G. Siu and Paul K. Chu
*Department of Physics and Materials Science, City University of Hong Kong, Kowloon, Hong Kong,
 People's Republic of China*

(Received 20 June 2005; accepted 15 November 2005; published online 3 January 2006)

A low-frequency Raman vibration mode, whose peak position and linewidth are independent of the sizes of Ge nanocrystals and the polarization configuration of incident excitation light, was observed in silicon oxide films embedded with Ge nanocrystals which were prepared using magnetron cosputtering of SiO₂-Ge-Si targets. The peak position of the Raman mode is sensitive to the content of Si in the matrix. After the sample is annealed above a special temperature that increases with the content of Si, the Raman mode disappears. Microstructural observations and spectral analyses disclose that this low-frequency Raman mode arises from a local structure which is positioned at the surfaces of Ge nanocrystals and consists of Ge, Si, and O atoms. High-temperature annealing leads to the removal of Ge atoms from the local structure. As a result, the local vibration mode vanishes. © 2006 American Institute of Physics. [DOI: 10.1063/1.2150594]

I. INTRODUCTION

Since the discovery of high efficient photoluminescence from porous Si,¹ various types of Si, Ge, and Si_{1-x}Ge_x nanostructures (nc-Si, nc-Ge, and nc-Ge_{1-x}Si_x) have intensively been studied. Particle sizes and surface structures have been shown to be the most important factors that decide optical properties and light-emitting efficiencies of these nanostructural materials. As potential light-sources at the nanometer scale, these nanostructures are usually embedded in a transparent silicon oxide matrix.

In the past decade, low-frequency Raman scattering has widely been used to study the particle size distribution and the coupling between the particle and matrix according to the vibration theories of acoustic phonons confined in nanoparticles.²⁻⁵ An inversely-proportional relationship between the vibration frequency and particle diameter was often reported.

Up to now, many experiments have shown that the low-frequency vibration characters of nc-Si and nc-Ge are strongly dependent upon the sample preparation conditions which directly determine the surface structure of nanoparticles.⁶⁻¹⁰ Our recent work also disclosed that the low-frequency vibrations of nc-Ge, nc-Si, and nc-Ge_{1-x}Si_x in silicon oxide depend on the coupling between nanocrystals and the matrix.¹¹ However, the influence of the matrix on the vibration properties of nanocrystals is sophisticated and still far from clearness.^{12,13} This is especially the case for Ge nanocrystals embedded in the matrix. Therefore, more experimental and theoretical studies are needed to address this problem. In this paper, we report a new phenomenon in the low-frequency Raman scattering of silicon oxide films em-

bedded with Ge nanocrystals. A low-frequency Raman peak is observed. Its frequency and linewidth are independent of the particle size of nc-Ge and the polarization configuration of incident light. Spectral analyses reveal that the Raman mode arises from a local structure which is composed of Ge, Si, and O atoms and distributes at the surface of nc-Ge in the silicon oxide matrix.

II. SAMPLES AND EXPERIMENTAL METHOD

The samples used in this work were prepared using radio-frequency magnetron cosputtering of SiO₂-Ge-Si targets and postannealing processing. This method has previously been used to fabricate nc-Ge-, nc-Si-, or nc-Ge_{1-x}Si_x-embedded silicon oxide films.¹¹ In our current experiments, some Ge and Si chips were placed on a large silica target and cosputtered under the conditions of 1 Pa Ar gas, 140 W power, and room temperature. The area ratios of Ge and Si chips to silica target are $P_{\text{Ge}}=4\%$ and $P_{\text{Si}}=2\%$. The fabricated film is a sandwich structure, SiO₂/SiO₂:Ge:Si/SiO₂. The up and down layers are about 40 nm in thickness. The thickness of the sandwiched layer is about 3 μm. The substrate is a <100>-oriented *c*-Si wafer. The deposited films were then annealed at the temperatures ranging from 700 to 1100 °C in N₂ ambient for 30 min. All the samples were characterized using high-resolution transmission electron microscope (HRTEM, CM200ST/FEG), x-ray diffraction (XRD, Rigaku D/max-RA type powder diffractometer using Cu Kα radiation) and Fourier-transform infrared absorption spectra (FTIR, NEXUS870). Raman spectra were obtained on a T64000 triple Raman system at backscattering geometry using the 514.5 nm line of the Ar-ion laser as an excitation source. Two different configurations were employed, with the excitation and detection po-

^{a)}Author to whom correspondence should be addressed; electronic mail: hxxlwu@nju.edu.cn

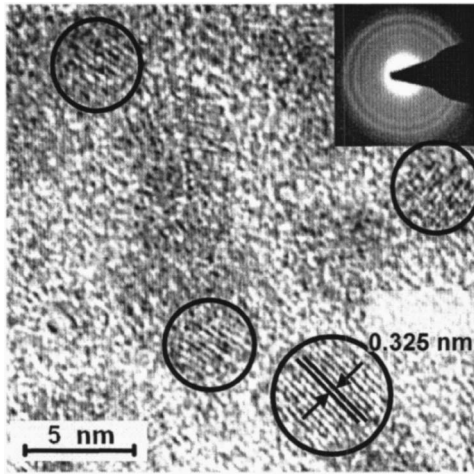


FIG. 1. High-resolution TEM image of the nanocrystal-embedded silicon oxide film. The inset is the selected area electron diffraction pattern.

larizations either parallel (polarized) or perpendicular (depolarized) to each other. All the measurements are run at room temperature.

III. RESULTS AND DISCUSSIONS

Figure 1 shows a typical HRTEM image of the nanocrystal-embedded film annealed at 950 °C. We can see that the nanocrystals are generally spherical in shape and have random orientation, because the selected area electron diffraction pattern clearly shows two dispersive diffraction rings (see the inset of Fig. 1). The marked spacing between the lattice fringes in the image is measured to be about 0.325 nm, which corresponds to the spacing between the (111) planes of nc-Ge. These TEM observations indicate that the average particle size is about 5 nm.

To compare with our current experimental results, we first take a look at our previous depolarized Raman spectra of nc-Ge and nc-Ge_{1-x}Si_x embedded in the silicon oxide films.¹¹ Figure 2(a) is the Raman results from the samples fabricated under the condition of $P_{\text{Ge}}=4\%$ and $P_{\text{Si}}=0\%$. The Raman peak at about 300 cm⁻¹ corresponds to the TO/LO phonon mode of nc-Ge. Figure 2(b) is the Raman results from the samples fabricated under the condition of $P_{\text{Ge}}=4\%$ and $P_{\text{Si}}=6\%$. The Raman peaks at about 290, 410, and 480 cm⁻¹ correspond to the Ge-Ge, Ge-Si, and Si-Si local optical phonon modes of nc-Ge_{1-x}Si_x ($x \sim 0.46$), respectively. The sharp peak at 521 cm⁻¹ is from the TO/LO phonon of the *c*-Si substrate. It is obvious that with increasing annealing temperature, nc-Ge and nc-Ge_{1-x}Si_x grow up quickly. In each spectrum of Figs. 2(a) and 2(b), an asymmetrical Raman peak appears in the low-frequency region. With the particles growing up, the low-frequency peak redshifts and becomes narrower in linewidth. This is a typical behavior of an acoustic phonon vibration mode confined in nanocrystals. In each polarized Raman spectrum (not shown), there is a similar low-frequency peak whose position is at a slightly higher frequency. It can be attributed to another confined acoustic phonon vibration mode.¹¹

Figures 2(c) and 2(d) respectively show the depolarized and polarized Raman spectra of the sandwich structures pre-

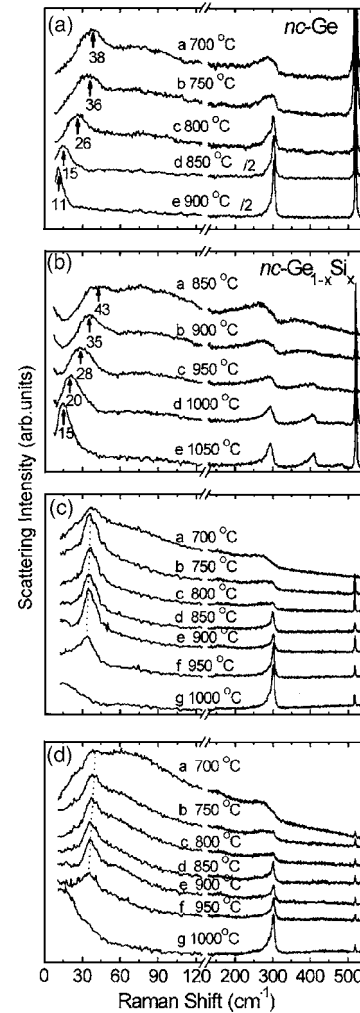


FIG. 2. Raman spectra of nc-Ge or nc-Ge_{1-x}Si_x ($x \approx 0.46$) embedded in the silicon oxide films, taken under excitation with the 514.5 nm line of the Ar⁺ laser at backscattering geometry and at room temperature. (a) $P_{\text{Ge}}=4\%$, $P_{\text{Si}}=0\%$, depolarized configuration; (b) $P_{\text{Ge}}=4\%$, $P_{\text{Si}}=6\%$, depolarized configuration; (c) $P_{\text{Ge}}=4\%$, $P_{\text{Si}}=2\%$, depolarized configuration; (d) $P_{\text{Ge}}=4\%$, $P_{\text{Si}}=2\%$, polarized configuration.

pared under the current condition of $P_{\text{Ge}}=4\%$ and $P_{\text{Si}}=2\%$. It can clearly be seen that for the depolarized and polarized configurations, only the signal from Ge-Ge optical phonon appears in the high-frequency region of each Raman spectrum. Thus, we can infer that the formed nanocrystals are nc-Ge. However, for the present samples, the low-frequency Raman spectra are completely different from those in Figs. 2(a) and 2(b), displaying the following features: (1) With increasing the particle size (that is, increasing annealing temperatures from 700 to 950 °C), the peak position only slightly shifts down from 38 to 35 cm⁻¹ and no noticeable linewidth narrowing is observed; (2) The existence of this Raman peak is independent of the selected polarization configuration; (3) This low-frequency peak disappears in the samples annealed over 1000 °C.

Since the vibration frequency and linewidth of this Raman mode are almost independent of the particle sizes, we can exclude the mode to be from any acoustic phonon vibration confined in nc-Ge with either free surface or fixed surface. We found that under excitation with the 632 nm line of

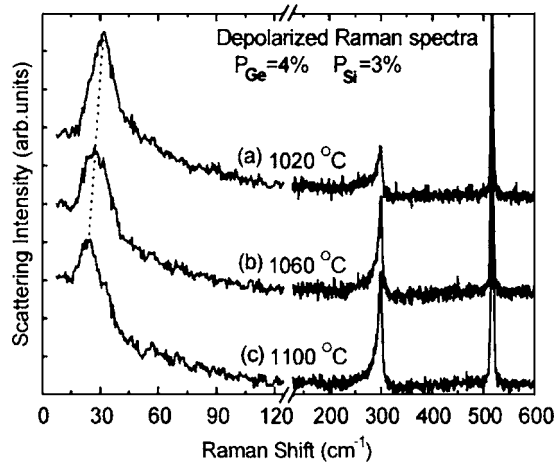


FIG. 3. Depolarized Raman spectra of the silicon oxide films prepared under the condition of $P_{\text{Ge}}=4\%$, $P_{\text{Si}}=3\%$.

the He–Ne laser, this low-frequency Raman mode still exists at the same position. Therefore, it is not also a luminescence line. In addition, we can further rule out this vibration mode to be the Boson peak of amorphous SiO_2 , which is very broad.¹⁴ Based on the above mentioned features of this low-frequency Raman mode, we infer that it may arise from some kind of local structure, which is related to both Ge and Si atoms, because no similar low-frequency vibration mode was observed in the Raman spectra of pure silica, Si-doped silica, and Ge-doped silica.

To give more information about this local structure, we prepared another group of samples with Si contents slightly higher ($P_{\text{Si}}=3\%$). The depolarized Raman spectra of some annealed samples are shown in Fig. 3. We can see that the formed nanocrystals are still nc-Ge, but the low-frequency vibration mode has not vanished in the samples annealed over 1000 °C. In the sample annealed at 1100 °C, although the position of this peak has shifted to 26 cm^{-1} , its shape and linewidth have no evident variation compared with those from the samples annealed at lower temperatures and from the samples prepared at $P_{\text{Si}}=2\%$. Thus, we can infer that the low-frequency Raman mode from the two groups of samples ($P_{\text{Si}}=3\%$ and $P_{\text{Si}}=2\%$) originates from a similar local structure. The vibration frequency of this kind of local structure is sensitive to the content of Si in the matrix.

To identify the position of the local structure in the film, we prepared more samples under the condition of $P_{\text{Ge}}=1\%$ and $P_{\text{Si}}=2\%$. The depolarized spectra of the samples annealed at 1000, 850, and 700 °C are displayed in Figs. 4(b)–4(d). It is obvious that no nc-Ge was formed in the three annealed samples. Since our experiments have indicated that more Ge introduction ($P_{\text{Ge}}>1\%$) would cause significant segregation of excessive Ge atoms to form nc-Ge [see Fig. 4(a)], there should be enough Ge atoms to be involved in the special local structure. Considering such a fact that the samples without nc-Ge do not show the low-frequency Raman vibration mode, we may infer that the local structure should exist at the surface of nc-Ge.

Below we discuss thermal stability of the local structure. Because the contents of both Ge and Si in our current silicon oxide films are very low, the infrared absorption spectra of

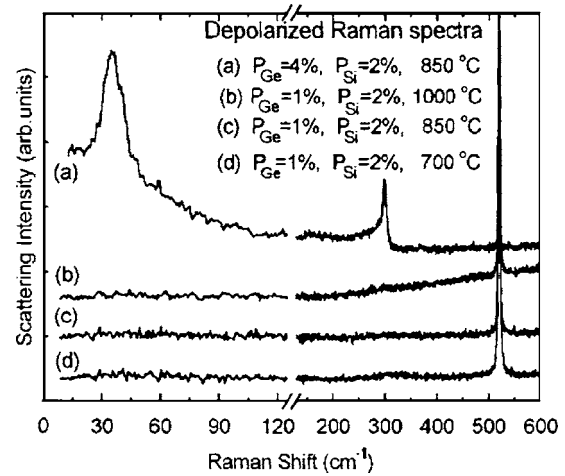


FIG. 4. Depolarized Raman spectra of the silicon oxide films prepared under condition of $P_{\text{Ge}}=1\%$ and $P_{\text{Si}}=2\%$ [spectra (b)–(d)]. Spectrum (a) is from the silicon oxide film prepared under the condition of $P_{\text{Ge}}=4\%$, $P_{\text{Si}}=2\%$ and $T_a=850\text{ °C}$.

all the Ge- or Si-doped samples are quite similar to that of amorphous silicon dioxide ($a\text{-SiO}_2$). It has been well known that in $a\text{-SiO}_2$ the Si–O–Si bond has three infrared absorption peaks at about 1095, 808, and 465 cm^{-1} , corresponding to the asymmetric stretching, bending, and rocking vibrations, respectively.¹⁵ Table I shows the peak positions of the three absorption bands from the samples prepared under $P_{\text{Ge}}=4\%$ and $P_{\text{Si}}=2\%$. It can be seen that with increasing annealing temperature, their peak positions gradually shift to those of $a\text{-SiO}_2$. In the sample annealed at 1050 °C, their positions are consistent with those of $a\text{-SiO}_2$. This means that almost all excessive Ge and Si atoms have segregated into nanocrystals from the matrix at such a high temperature. This is accompanied with removal of the local structure. The thermal behavior confirms that the local structure is Si rich.

By comparing the intensity and width of optical phonon modes in the samples with and without Si doping, we have also found that the doping of Si has an effect of limiting nc-Ge growth. This means that excessive Si atoms can suppress the diffusion of Ge atoms in the matrix, which may be responsible for the improved thermal stability of the local structure when the content of Si increases from $P_{\text{Si}}=2\%$ to 3% (see Fig. 3). In addition, with increasing annealing temperature, excessive Ge atoms segregate to form nc-Ge. For

TABLE I. The vibration frequencies of the Si–O–Si bond in the FTIR absorption spectra of $a\text{-SiO}_2$ and nc-Ge films prepared under the condition of $P_{\text{Ge}}=4\%$, $P_{\text{Si}}=2\%$. The data in parentheses is the error of peak frequency, which is estimated based on the sharpness of the absorption peak.

Sample preparation conditions	Vibrational frequencies of Si–O–Si bond		
	Asymmetric stretching ($\pm 5\text{ cm}^{-1}$)	Bending ($\pm 1.5\text{ cm}^{-1}$)	Rocking ($\pm 2\text{ cm}^{-1}$)
$a\text{-SiO}_2$ 900 °C	1093.9	808.0	466.7
$P_{\text{Ge}}=4\%$, $P_{\text{Si}}=2\%$, 1050 °C	1097.3	807.6	465.5
$P_{\text{Ge}}=4\%$, $P_{\text{Si}}=2\%$, 900 °C	1089.6	812.5	460.6
$P_{\text{Ge}}=4\%$, $P_{\text{Si}}=2\%$, 750 °C	1085.6	814.4	457.6

the samples with excessive Si atoms, however, no nc-Si or nc-Ge_{1-x}Si_x was detected from the Raman scattering results. We guess that one possible segregation process of excessive Si atoms is to form a Si-rich outer shell of nc-Ge, as in the case with higher contents of Ge and Si.^{16,17} But such a nanocrystal model with Ge-Si shell or amorphous Si shell cannot explain the damage of the local structure at high temperature, because this model will result in a heavier alloying of Ge and Si nanocrystals at high temperature.¹⁷ In fact, the alloying phenomenon has not taken place in our current samples.

Based on the above experimental results, we infer that the local structure may be a Si-rich GeSiO ternary complex, which exists between Ge core and the silicon oxide matrix. Such a ternary interlayer is helpful for decreasing stress energy between nc-Ge and the silicon oxide matrix and can be responsible for the disappearance of the confined surface acoustic phonon modes in the present samples. According to the elastic continuum approximation, the reflection of sound waves at the interface is negligible when the acoustic impedances for the nanocrystal and the matrix match.¹⁸ Acoustic impedance for Ge is about 2.14 times that of silica. The doping of both Si and Ge would obviously increase the acoustic impedance of the silicon oxide matrix. Therefore, when the acoustic impedance of the interlayer is close to that of the Ge nanocrystal, the confined acoustic vibration disappears. Since the interface layer is very complicated in structure, so far it is still difficult to give an exact model theoretically describing the local structure based on current experimental results. Further work is needed to address this issue from theory.

It is interesting to mention that in borosilicate glass embedded with CdSe nanocrystals, Saviot *et al.*¹⁹ have also observed a narrow line whose position was near 38 cm⁻¹ and almost independent of particle sizes. They believe that this narrow line cannot be related to any confined acoustic mode. They noticed that the energy of this line is close to the bulk band edge TA phonon energy and close to bulk E₂ optical mode energy in wurtzite CdSe. However, their explanation cannot be adopted to describe our experimental result. The reason is that the phonon spectrum of bulk Ge is different from that of wurtzite CdSe. In addition, the narrow line in our experiment disappears at high temperature. Most importantly, the frequency of the narrow line is sensitive to the content of Si, although the formed nanocrystals are still nc-Ge. Therefore, we believe that the low-frequency Raman mode in our experiment is from a local vibration in the interlayer.

IV. CONCLUSIONS

We have investigated the origin of a low-frequency Raman vibration mode in the Raman spectra of silicon oxide

films embedded with nc-Ge. The peak position and linewidth of this vibration mode are independent of the size of nc-Ge and the polarization configuration of incident light. The vibration frequency is sensitive to the content of the doped Si atoms in the matrix. Our experiments reveal that this vibration mode arises from a local structure, which is composed of Ge, Si, and O atoms and is positioned at the surface of nc-Ge. This local structure would break down after the samples are annealed at a high temperature due to annealing out of Ge atoms from this structure. This work will be beneficial for further investigations on the low-frequency phonon property of nc-Ge in the silicon oxide matrix.

ACKNOWLEDGMENTS

This work was supported by the Grants (Nos. 10225416, 60476038, and 60576061) from the National Natural Science Foundation of China and the LAPEM. Partial support was also from the Major State Basic Research Project No. G001CB3095 of China and City University of Hong Kong Direct Allocation Grant No. 9360110.

¹A. G. Cullis and L. T. Canham, *Nature* (London) **353**, 335 (1991).

²A. Dieguez, A. Romano-Rodriguez, J. R. Morante, N. Barsan, U. Weimar, and W. Gopel, *Appl. Phys. Lett.* **71**, 1957 (1997).

³E. Duval, H. Portales, L. Saviot, M. Fujii, K. Sumitomo, and S. Hayashi, *Phys. Rev. B* **63**, 075405 (2001).

⁴P. Verma, W. Cordts, G. Irmer, and J. Monecke, *Phys. Rev. B* **60**, 5778 (1999).

⁵D. B. Murray and L. Saviot, *Phys. Rev. B* **69**, 094305 (2004).

⁶M. Fujii, Y. Kanzawa, S. Hayashi, and K. Yamamoto, *Phys. Rev. B* **54**, R8373 (1996).

⁷X. L. Wu, G. G. Siu, X. Y. Yuan, N. S. Li, Y. Gu, X. M. Bao, S. S. Jiang, and D. Feng, *Appl. Phys. Lett.* **73**, 1568 (1998).

⁸X. L. Wu, Y. F. Mei, G. G. Siu, K. L. Wong, K. Moulding, M. J. Stokes, C. L. Fu, and X. M. Bao, *Phys. Rev. Lett.* **86**, 3000 (2001).

⁹L. Saviot, D. B. Murray, and M. D. M. de Lucas, *Phys. Rev. B* **69**, 113402 (2004).

¹⁰N. N. Ovsiuk and V. N. Novikov, *Phys. Rev. B* **53**, 3113 (1996).

¹¹Y. M. Yang, X. L. Wu, L. W. Yang, G. S. Huang, G. G. Siu, and P. K. Chu, *J. Appl. Phys.* **98**, 064303 (2005).

¹²N. Daldosso, M. Luppi, S. Ossicini, E. Degoli, R. Magri, G. Dalba, P. Fornasini, R. Grisenti, F. Rocca, L. Pavesi, S. Boninelli, F. Priolo, C. Spinella, and F. Iacona, *Phys. Rev. B* **68**, 085327 (2003).

¹³G. Hadjisavvas and P. C. Kelires, *Phys. Rev. Lett.* **93**, 226104 (2004).

¹⁴A. Fontana, F. Rossi, G. Carini, G. D. Angelo, G. Tripodo, and A. Bartolotta, *Phys. Rev. Lett.* **78**, 1078 (1997).

¹⁵V. B. Neustruev, *J. Phys.: Condens. Matter* **6**, 6901 (1994).

¹⁶A. Kolobov, H. Oyanagi, N. Usami, S. Toknimitsu, T. Hattori, S. Yamasaki, K. Tanaka, S. Ohtake, and Y. Shiraki, *Appl. Phys. Lett.* **80**, 488 (2002).

¹⁷Y. M. Yang, X. L. Wu, G. G. Siu, G. S. Huang, J. C. Shen, and D. S. Hu, *J. Appl. Phys.* **96**, 5239 (2004).

¹⁸D. B. Murray and L. Saviot, *Phys. Rev. B* **69**, 094305 (2004).

¹⁹L. Saviot, B. Champagnon, E. Duval, I. A. Kudriavtsev, and A. I. Ekimov, *J. Non-Cryst. Solids* **197**, 238 (1996).